



Morphological patterns of the rib cage and lung in the healthy and adolescent idiopathic scoliosis

Benedikt Schlager¹  | Florian Krump¹ | Julius Boettinger¹ | René Jonas¹ | Christian Liebsch¹ | Michael Ruf² | Meinrad Beer³ | Hans-Joachim Wilke¹ 

¹Institute of Orthopaedic Research and Biomechanics, Centre for Trauma Research Ulm, Ulm University Medical Centre, Ulm, Germany

²Skoliosechirurgie, Zentrum für Wirbelsäulenchirurgie, Orthopädie und Unfallchirurgie, SRH Klinikum Karlsbad-Langensteinbach gGmbH, Karlsbad, Germany

³Department of Diagnostic and Interventional Radiology, Ulm University Medical Center, Ulm, Germany

Correspondence

Hans-Joachim Wilke, Institute of Orthopaedic Research and Biomechanics, Centre for Trauma Research Ulm, Ulm University Medical Centre, Helmholtzstraße 14, 89081 Ulm, Germany.
Email: hans-joachim.wilke@uni-ulm.de

Funding information

Deutsche Forschungsgemeinschaft, Grant/Award Number: WI 1352/20-2 and WI 1352/22-1

Abstract

The morphology of the rib cage affects both the biomechanics of the upper body's musculoskeletal structure and the respiratory mechanics. This becomes particularly important when evaluating skeletal deformities, as in adolescent idiopathic scoliosis (AIS). The aim of this study was to identify morphological characteristics of the rib cage in relation to the lung in patients with non-deformed and scoliotic spines. Computed tomography data of 40 patients without any visible spinal abnormalities (healthy group) and 21 patients with AIS were obtained retrospectively. All bony structures as well as the right and left lung were reconstructed using image segmentation. Morphological parameters were calculated based on the distances between characteristic morphological landmarks. These parameters included the rib position, length, and area, the rib cage depth and width, and the rib inclination angle on either side, as well as the spinal height and length. Furthermore, we determined the left and right lung volumes, and the area of contact between the rib cage and lung. Differences between healthy and scoliotic spines were statistically analysed using the *t*-test for unpaired data. The rib cage of the AIS group was significantly deformed in the dorso-ventral and medio-lateral directions. The anatomical proximity of the lung to the ribs was nearly symmetrical in the healthy group. By contrast, within the AIS group, the lung covered a significantly greater area on the left side of the rib cage at large thoracic deformities. Within the levels T1–T6, no significant difference in the rib length, depth to width relationship, or area was observed between the healthy and AIS groups. Inferior to the lung (T7–T12), these parameters exhibited greater variability. The ratio between the width of the rib cage at T6 and the thoracic spinal height (T1–T12) was significantly increased within the thoracic AIS group (1.1 ± 0.08) compared with the healthy group (1.0 ± 0.05). No statistical differences were found between the lung volumes among all the groups. While the rib cage was frequently strongly deformed in the AIS group, the lung and its surrounding ribs appeared to be normally developed. The observed rib hump in AIS appeared to be formed particularly by a more ventral position of the ribs on the concave side. Furthermore, the rib cage width to spinal height ratio suggested that the spinal height of the thoracic AIS-spine

This is an open access article under the terms of the Creative Commons Attribution-NonCommercial-NoDerivs License, which permits use and distribution in any medium, provided the original work is properly cited, the use is non-commercial and no modifications or adaptations are made.

© 2021 The Authors. *Journal of Anatomy* published by John Wiley & Sons Ltd on behalf of Anatomical Society.

is reduced. This indicates that the spine would gain its growth-related height after correcting the spinal deformity. These are the important aspects to consider in the aetiology research and orthopaedic treatment of AIS.

KEYWORDS

AIS, biomechanics, chest, lung, morphology, rib cage, scoliosis, thorax

1 | INTRODUCTION

The morphology of the rib cage affects both the biomechanics of the upper body's musculoskeletal structure and the respiratory mechanics (Sanchis-Gimeno et al., 2020). Analysing the shape of the thorax is particularly relevant in the case of skeletal deformities, as in adolescent idiopathic scoliosis (AIS). This can provide information on AIS aetiology (Stokes et al., 1989) and orthopaedic treatment (Harris et al., 2014), as well as on potential respiratory impairment (Yaszay et al., 2017).

The bone in the scoliotic spine exhibits characteristic morphological patterns (Schlager et al., 2018), which is explained by an asymmetrical loading governed by the Hueter-Volkman principle (Stokes et al., 1996). Morphological patterns indicate a pathological growth development, which may be an indication for the inherent biomechanical loading condition of the spine and thorax. While the morphology of the spine has been extensively investigated (Parent et al., 2002; Schlager et al., 2018), a systematic analysis of the rib cage and lung morphology in relation to the spinal curvature is currently lacking.

1.1 | Development of the healthy rib cage

During the embryonic period, the dimensions of the rib cage are dominated by the growth of the abdominal organs (Okuno et al., 2019). Postnatally, the chest shape further adapts to the pulmonary function (Bastir et al., 2013; Grivas, 1991). Generally, the adult-like thoracic shape is attained at the end of the second postnatal year (Openshaw et al., 1984). With increasing age from childhood to adulthood, the rib cage increases in magnitude and the inclination angle of the ribs gradually increases caudally (Gayzik et al., 2008; Holcombe et al., 2017).

The rib cage increases the stiffness of the thoracic spine, almost doubling the thoracic spinal stability in axial rotation (Liebsch et al., 2017; Liebsch & Wilke, 2020). Furthermore, its motion accounts for approximately 35%–50% of the vital capacity of the lung in healthy subjects (Eberlein et al., 2014). During spinal motion, the rib cage structures undergo large range of motions but small deformations (Liebsch et al., 2019). The influence of the rib cage dimensions on thorax stiffness is currently unknown.

1.2 | Rib cage morphology within AIS

Patients with AIS can exhibit a prominent thoracic deformity, with a rib hump on the convex side of the spine (Closkey & Schultz, 1993;

Harris et al., 2014; Labelle et al., 1995; Stokes et al., 1989). The shape of the spinal curvature in AIS is related to the shape of the rib cage (Grivas et al., 2007) and the lung capacity (Dreimann et al., 2014).

Large deformities are accompanied by restricted kinematic movement of the rib cage, whereas the motion of the diaphragm appears to be unaffected (Kotani et al., 2004; Leong et al., 1999). AIS has been generally associated with a decrease in total lung capacity, which manifests particularly at a Cobb-angle above 70° (Kearon et al., 1993). Although it has been reported that mild AIS cases also demonstrate an impairment of the ventilatory function (Abdelaal et al., 2018; Smyth et al., 1984), no clear correlation between morphological deformity of the spine and the lung vital capacity (Kearon et al., 1993) or between the rib cage volume and pulmonary function has been observed (Bouloussa et al., 2019).

Statistically significantly longer rib lengths on the concave side were observed from the 8th to 12th rib (Kasai et al., 2002; Qiu et al., 2010; Stokes et al., 1989). No difference in the rib lengths between the left and right sides were reported for the upper seven ribs. The discrepancy of the rib length appears to be secondary, not primary, to the cause of AIS (Zhu et al., 2011).

A variety of further parameters were introduced for surgical planning to describe the thoracic deformity, particularly in planar radiographs (Harris et al., 2014). An understanding of the overall development of spinal deformity, rib cage formation, and lung formation currently remains lacking.

These findings demonstrate that the relationship between the deformed spine, the rib cage morphology, and pleural mechanics is complex. Despite this, we hypothesise that the morphology of the rib cage is strongly associated with the spine. To clarify the overall relationship, various morphological parameters, including lung mechanics, need to be considered.

In this study, we systematically analysed various morphological parameters to depict the overall relationship between the spinal curvature, rib cage, and lung.

This morphological data may provide an insight into the basic structure of the healthy rib cage, as well as to the pathology of AIS. The morphological data of the rib cage is further relevant for biomechanical models, because its shape may influence the thoracic stiffness and the respiratory movement.

2 | METHODS

Morphological parameters of the spine and rib cage were obtained by evaluating computed tomography (CT) images of 21 patients

diagnosed with AIS ("AIS" group) and 40 patients without any visible spinal abnormalities ("healthy" group). The mean age was 15 ± 2 years for the AIS group and 23 ± 12 years for the healthy group. All CT data were obtained retrospectively from the radiology departments; therefore, no CT images were taken for this study (Ethical votes 418/15-Zo/Sta, B-F-2016-053). Inclusion criteria for the CT data were a slice thickness of ≤ 1 mm and visibility of the spinal levels T1 to S1, including the entire thorax. To reduce data variability, the AIS cases were subdivided into three groups depending on the type of scoliotic curvature (Figure 1): lumbar ($n = 5$, mean lumbar Cobb-angle 54° , min. 45° - max. 72°), thoracic ($n = 12$, mean thoracic Cobb-angle 64° , min. 37° - max. 101°) and thoracolumbar ($n = 4$, mean thoracic Cobb-angle 97° , min. 68° - max. 117°). All thoracic curvatures were right convex and lumbar curvatures left convex.

The bony structures as well as the volume of the lung on the left and right thorax sides were manually reconstructed from the CT scans using the software tool AVIZO (release: 8.0; FEI Visualization Sciences Group). Landmarks were placed manually on predefined characteristic morphological points on the spine and rib cage (Figure 1). These landmarks were: a point on the posterior position (postRib), medial position (medRib), and anterior position (antRib) of the respective rib, as well as the posterior point on the superior endplate of the vertebral body (supVert). Morphological parameters were derived from the coordinates of the respective landmarks.

2.1 | Morphological parameters

Firstly, the position of the landmarks was referred to a patient-specific coordinate system which was defined by S1, T1, and the suprasternal notch, with the origin at S1 and the caudo-cranial axis running through T1 (Figure 1).

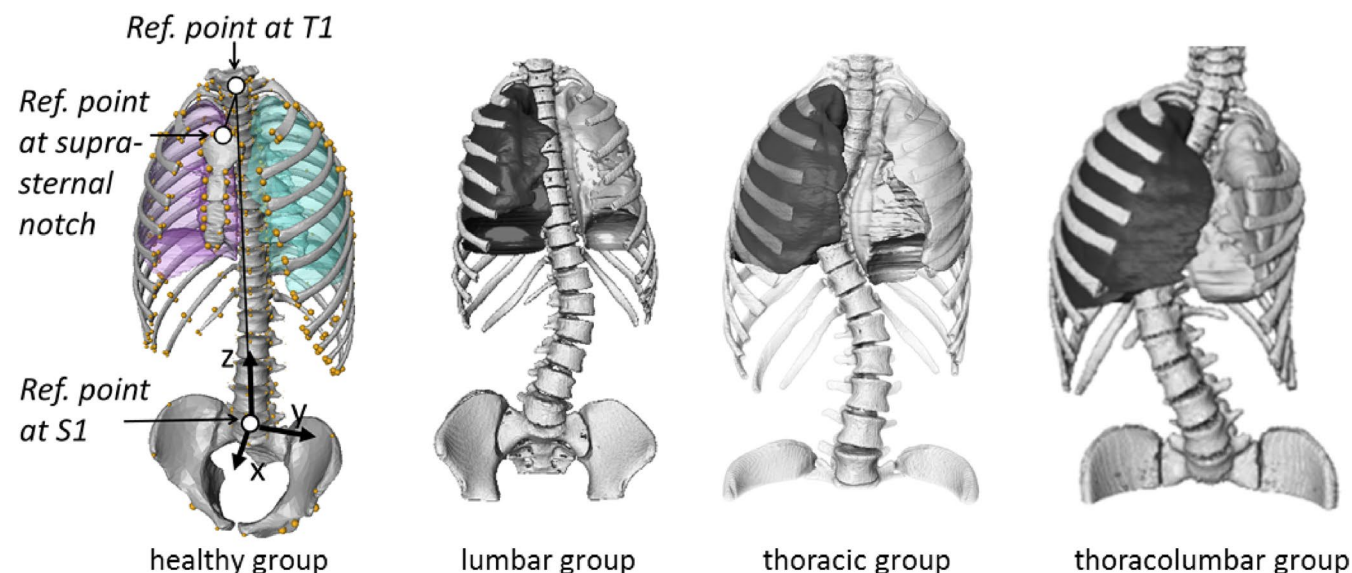


FIGURE 1 Illustration of the global coordinate system defined by S1–T1 and the middle of the suprasternal notch as well as the position of the landmarks (extreme left). Exemplary patient cases of the three different spinal groups (right)

Using the 3D-coordinates of the landmarks, the following parameters were derived (Figure 2):

- **Posterior** position of each rib: location of the postRib-landmark in the dorso-ventral direction within the patient-specific coordinate system
- **Medial** position of each rib: location of the medRib-landmark in the medio-lateral direction within the patient-specific coordinate system
- **Anterior** position of each rib: location of the antRib-landmark in the dorso-ventral direction within the patient-specific coordinate system
- **Length** of each rib: length of a line connecting the landmarks supVert, postRib, medRib, and antRib
- **Area covered by the rib**: area enclosed by the line connecting the four landmarks supVert, postRib, medRib, and antRib
- **Depth** of the rib cage: length of the line connecting the landmark supVert with the point in between the left and right antRib-landmarks
- **Width** of the rib cage: length of the line connecting the left and right medRib-landmarks
- **Inclination angle** of each rib: The rib numbers 1–12 were respectively associated to the adjacent thoracic levels 1–12.

The volume of the reconstructed lung was calculated based on the voxel mesh using AVIZO.

The area of contact between the lung and rib cage on the left and right sides was quantified (Figure 3). To accomplish this, the outer surface of the segmented pleura volume was converted into a shape of 2500 nodes and triangles, and exported into an STL-file format to obtain the dimensions of each lung. The smallest distance between the outer surface of the lung and landmarks at the anterior, middle, and posterior sections of the ribs was calculated. To determine

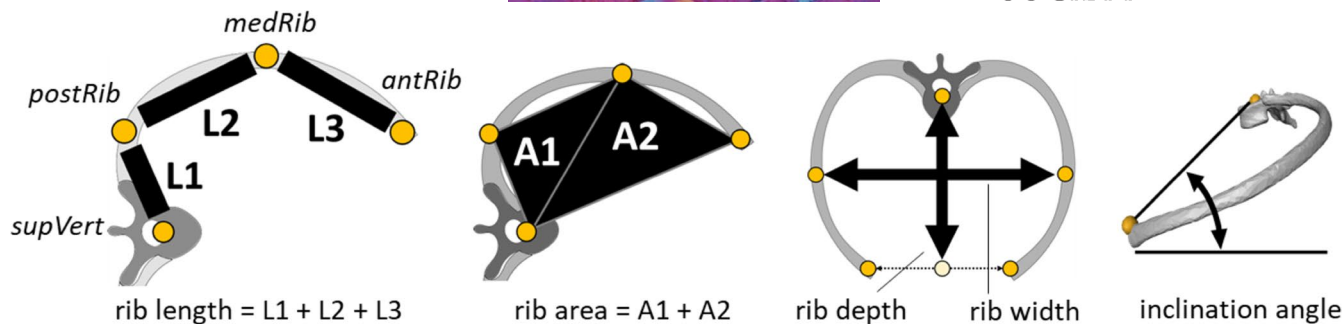


FIGURE 2 Morphological parameters calculated from the landmark locations. Landmarks were placed on the posterior position (postRib), medial position (medRib), and anterior position (antRib) of the respective rib, as well as the posterior point on the superior endplate of the vertebral body (supVert). Derived morphological parameters were rib length, area enclosed by the rib, depth and width of each rib level, inclination angle of the ribs. The inclination angle is the angle of the vector, pointing from the vertebral body to the anterior part of the rib and to the transverse plane of the global coordinate system

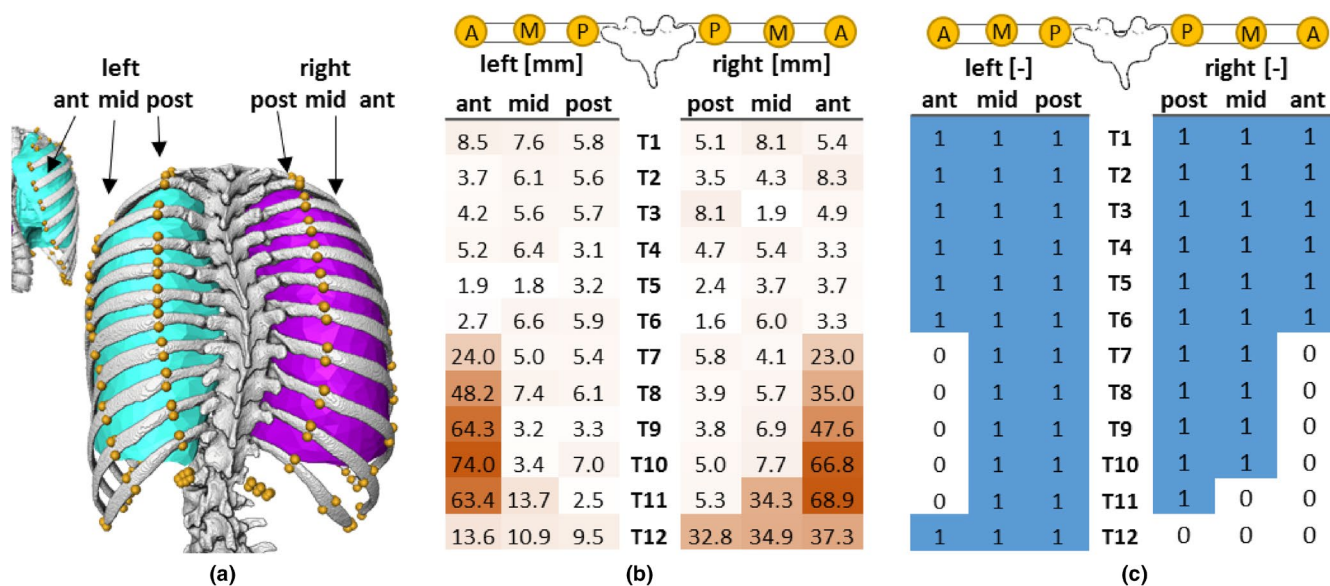


FIGURE 3 Example that illustrates how the anatomical proximity of the lung to the ribs was determined. (a) Patient case with the segmented bone and lung, as well as the position of the landmarks (yellow dots) on each rib in the posterior (post), middle (mid), and anterior (ant) sections. (b) Calculated nearest distance in mm from each landmark to the lung. (c) Simplified illustration, whether contact between lung and rib is present. All calculated distances below 20 mm are considered as full contact (1) and above 20 mm as no contact (0)

whether the lung was attached to a rib region, a distance threshold level of 20 mm was chosen. Below this threshold, the rib region was assumed to be attached to the lung. This threshold level corresponded to an upper limit of the rib height. Therefore, it was assured that deviations of the position of a landmark along a rib height could be neglected.

It should be further noted that no information on the breathing status or expiratory lung volume of the patients was available when the CT image was taken.

2.2 | Statistical analysis

The intra- and inter-observer variability for the placement of the landmarks was analysed by two observers who repeated the

placement of the landmarks six times on a healthy and a scoliotic spine. This procedure allowed for the determination of measurement accuracy for each parameter.

To identify statistical differences between the parameters of the healthy and scoliotic morphology data, the mean values at each spinal level were compared using the t-test for unpaired data. A significance level of 0.01 was chosen. The statistical analysis was performed using the SciPy package (version 0.16.0) within Python (version 3.4.3) (Virtanen et al., 2020).

3 | RESULTS

In all patients, the skeletal structure and lung volumes could be reconstructed, all landmarks placed, and morphological parameters

calculated. The absolute inter- and intra-observer variability of the parameters was approximately 1.6 mm. The greater the distance between the landmarks, the lower was the percentage error.

To compare the deformity of the spine to the rib cage parameters, the lateral position of the vertebral bodies within the coronal plane was plotted for each AIS group (Figure 4a).

3.1 | Posterior rib position

Generally, in all scoliotic cases, a more ventral position of the left rib on the concave side of the spinal curvature was observed between T6 and T9. The region of T7-T9 of the thoracic AIS group displayed a significantly more ventral position of the posterior rib section on the left side (Figure 4b), and a more dorsal position on the right side (Figure 4c). Similar data, but much more pronounced, was obtained for the thoracolumbar AIS group.

3.2 | Middle rib position

The lumbar AIS group displayed no significant difference in the middle section of the rib cage on the left side, whereas on the right side, the ribs were more medially positioned in the lower thoracic region.

The thoracic and thoracolumbar AIS groups both exhibited significant deformities, particularly at the levels T6-T9: an increased medial position of the rib on the left side, and a more ventral placed rib on the right (Figure 4d,e).

3.3 | Anterior rib position

No strong statistically significant differences could be identified between the healthy and AIS groups in the anterior position of the rib in the dorso-ventral direction (Figure 4f,g). By trend, the rib on the

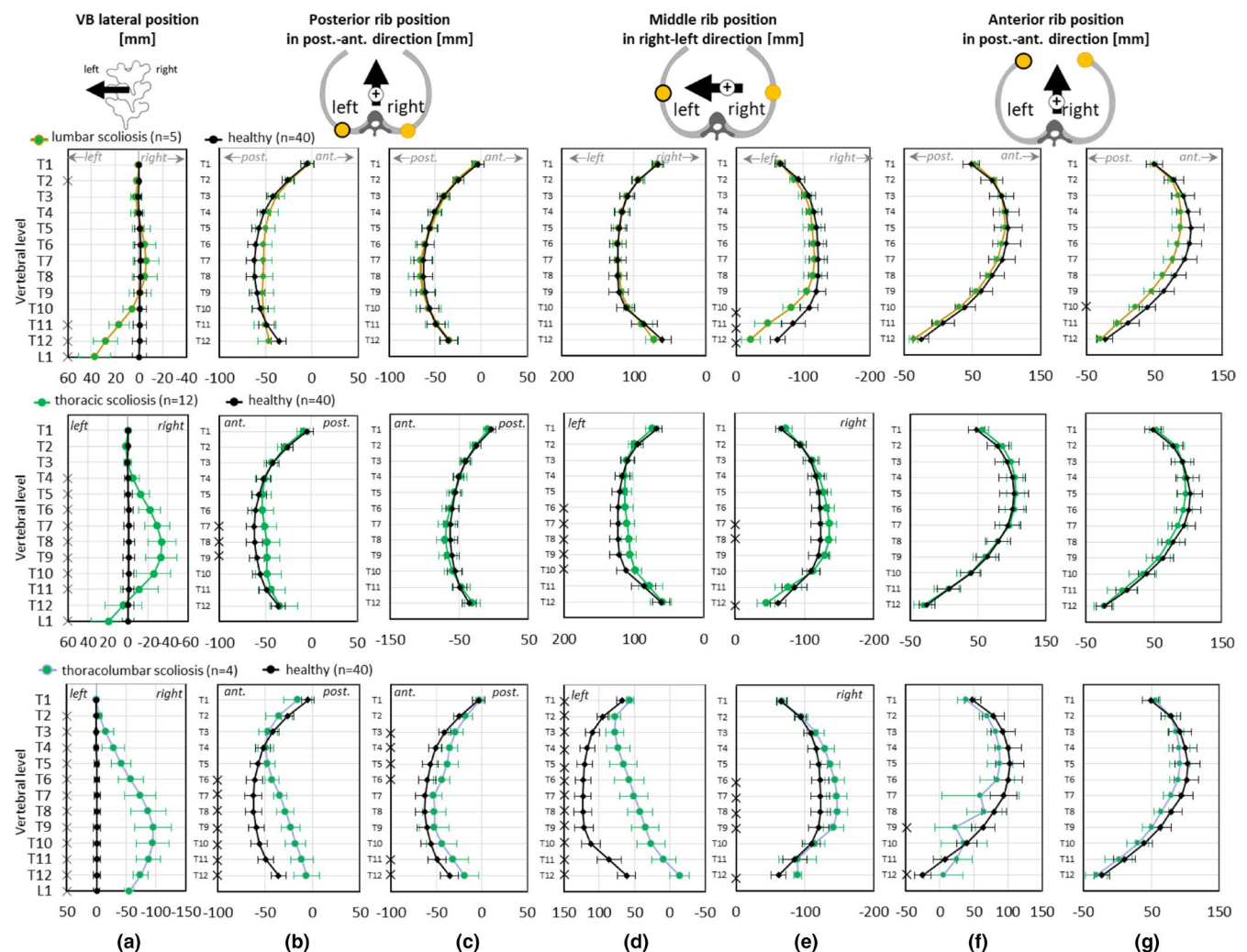


FIGURE 4 Morphological parameters of the healthy (black lines & dots) and scoliotic spines (coloured lines & dots): Lateral position of the vertebral bodies (VB) (a); dorso-ventral position of the posterior rib section on the left (b) and right (c) sides; medio-lateral position of the middle section of the left (d) and right (e) ribs; dorso-ventral position of the anterior rib section on the left (f) and right (g) sides; "x" indicates a p-value < 0.01 when comparing the AIS and healthy groups

right side was more dorsal at the levels T4–T8 within the lumbar and thoracic AIS groups.

3.4 | Lung volume

The mean lung volume was 3.0 L (0.9–6.5 L) in the healthy group, 3.2 L (1.2–5.3 L) in the lumbar AIS group, 2.9 L (1.4–4.1 L) in the thoracic AIS group, and 1.7 L (1.1–2.0 L) in the thoracolumbar AIS group. The volume of the left lung was generally less compared with the right lung (Figure 5a). No significant statistical differences were found between the spinal groups.

3.5 | Rib length relationship left to right side

The relationship between the length of the ribs on the left and right sides was for all groups close to 1.0 within the region of T1–T6, without any significant differences (Figure 6a). Commencing at T7, the rib length on the left side increased relative to the right side towards T11, particularly in the thoracic and thoracolumbar AIS groups.

3.6 | Rib depth to width

The lumbar and thoracic AIS groups did not display any significant differences between the depth and the width of the rib cage at each level in relation to the healthy group, aside from T1 within the thoracic group (Figure 6b). A significant increase in the relationship could be found within the thoracolumbar group in the levels T8–T11.

3.7 | Inclination angle of the ribs

The inclination angle of each rib, relative to the inclination angle of the rib at T1, tended to be greater for all AIS cases (Figure 6c,d). Significant differences were observed for the thoracic AIS-curvatures within the region T2–T8 and for the thoracolumbar curvatures within the complete lower thoracic region.

3.8 | Rib area left to right

The ribs enclosed nearly the same area on the left and right sides at the levels T1–T5 within all groups (Figure 6e). Commencing at T7 in the lumbar group and T6 in the thoracic group, the relationship between the areas increased significantly towards T11. At T12, a high standard deviation was obtained.

3.9 | The area of contact between the lung and rib cage

In the non-deformed (healthy) spine and rib cage, the contact area of the lung with the right and left sides was normally the same (Figure 5b). More than 80% of the ribs in the anterior rib region above T6, in the middle region above T8, and in the posterior region above T10 were attached to the lung.

By contrast, in the rib cage of AIS patients, the anatomical proximity of the lung to the ribs was reduced on the right (convex) side and increased on the left side. This asymmetry was significantly different at the levels T10–T12 in the mid-section of the rib on the left side for the thoracic and thoracolumbar AIS groups (Figure 6f).

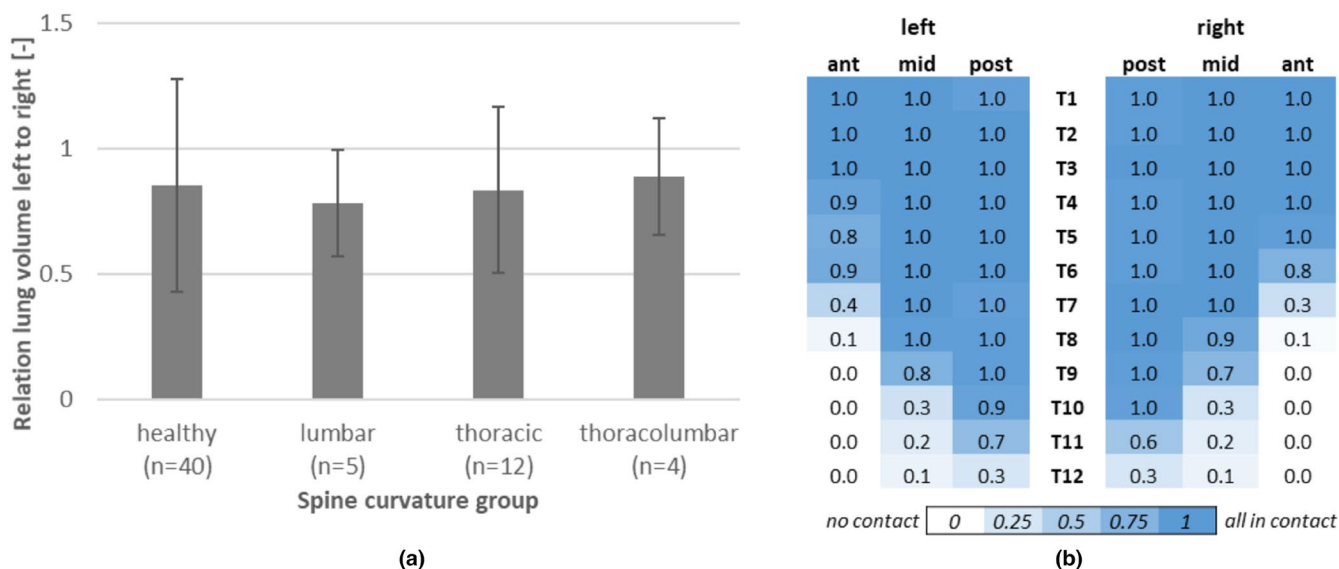


FIGURE 5 (a) Relationship between the left and right lung volumes for each type of spinal curvature (mean and standard deviation). (b) Average region of the rib cage that is in anatomical proximity of the lung for the non-deformed (healthy) spine group: anterior (ant), middle (mid), and posterior (post) regions of each rib. 0.0 indicates no contact (white) and 1.0 full contact within all subjects (blue) of the lung and rib in the specific region

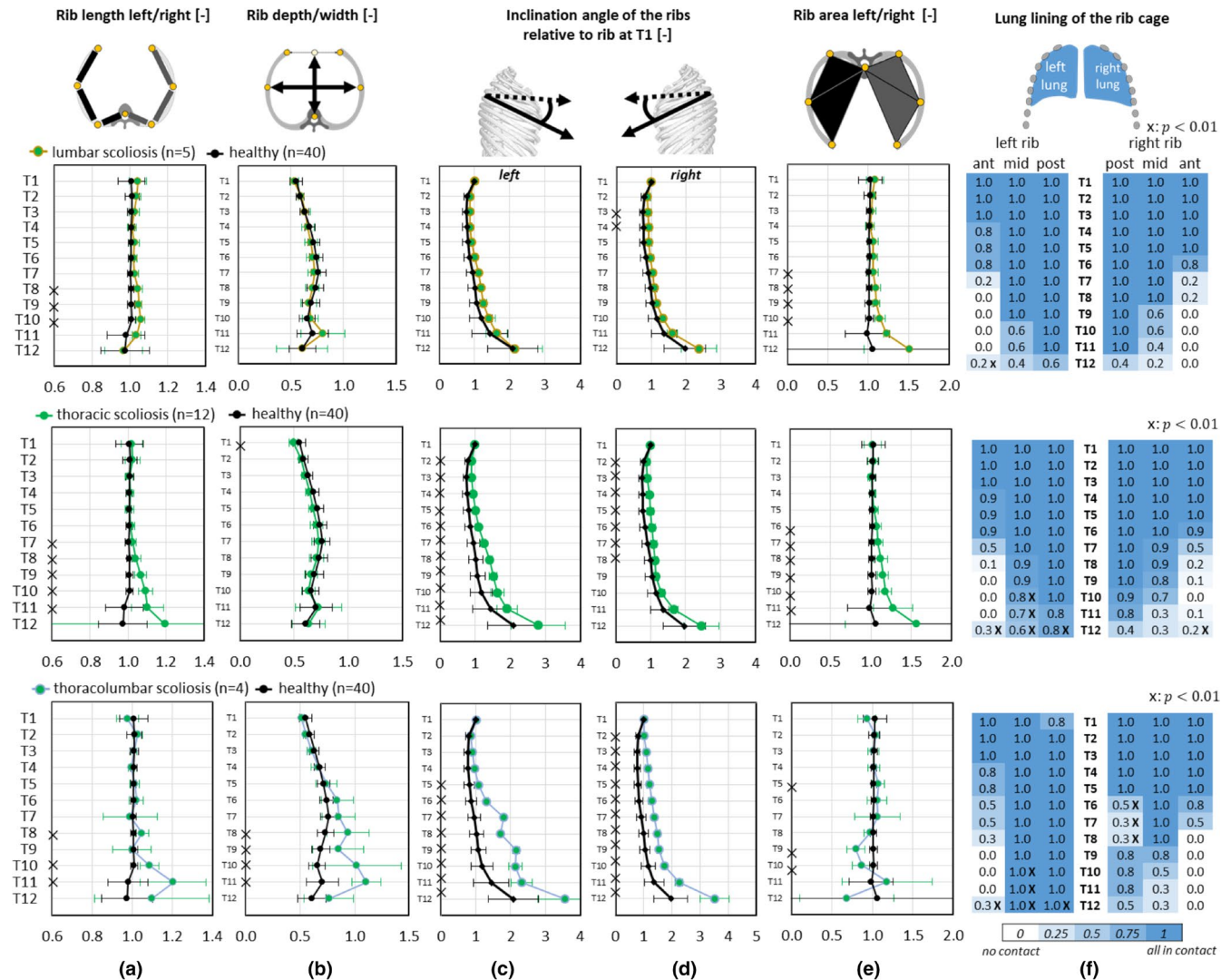


FIGURE 6 Morphological parameters of the healthy (black lines & dots) and scoliotic spines (coloured lines & dots): (a) Relationship between the left and the right rib lengths. (b) Relationship between the depth and the width of each rib level. (c) Inclination angle of the left and (d) right ribs relative to the inclination angle of T1. (e) Relationship between the left and right areas that are enclosed by the rib. (f) Anterior (ant), middle (mid), and posterior (post) rib regions which are attached to the lung; 0.0 indicates no contact (white) and 1.0 full contact within all subjects (blue) of the lung and rib in the specific region. "x" indicates a p -value $< .01$ when comparing the AIS and healthy groups

Furthermore, significant variations were observed at the levels T6–T8 on the right posterior rib section for the thoracolumbar group. Example CT images to visualise this offset are presented in the appendix (Figure A1).

3.10 | Relationship between the width of the rib cage and the spinal height and length

The relationship of the rib cage width at T6 with the spinal height ranging from T1 to T12 was, on average, 1.00 ± 0.05 (0.88–1.09) for the healthy group, 1.04 ± 0.08 (0.9–1.14) for the lumbar AIS group, 1.11 ± 0.09 (0.98–1.28) for the thoracic AIS group, and 1.04 ± 0.05 (1.01–1.12) for the thoracolumbar AIS group (Figure 7b). The two-sided unpaired t -test revealed a statistically significant difference between the thoracic AIS and healthy groups ($p < .001$).

4 | DISCUSSION

In this study, morphological characteristics of the deformed rib cage of AIS patients were compared with the non-deformed rib cage of patients without AIS. The data revealed that within the upper thoracic region, which was completely in contact with the lung, the rib cage of AIS patients displayed no fundamental morphological differences compared with the healthy rib cage. This included the length of the ribs, the area enclosed by the ribs, and the depth to width ratio of the ribs. Within the lower thoracic region, these parameters varied significantly.

4.1 | Rib length

An increased length of the ribs in AIS patients has also been reported in previous studies (Kasai et al., 2002; Stokes et al., 1989). Animal research

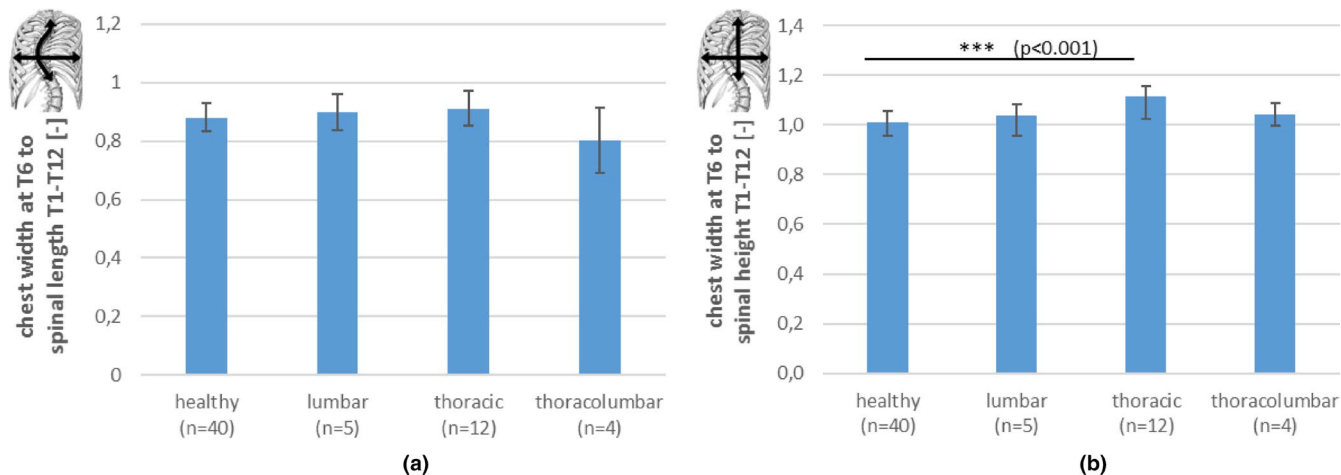


FIGURE 7 Relationship between the rib cage width, measured between the left and right medial points of the 6th rib, and the spinal length (a) and height (b). The spinal length was measured along the spinal curvature from T1 to T12 and the spinal height as the direct line between T1 and T12

suggested that asymmetrical growth of the rib length may be a cause for spinal deformity (Zhu et al., 2011). By contrast, the results of the present study are in agreement with the findings that the asymmetrical rib length and surface are limited to the lower thoracic region (Kasai et al., 2002; Qiu et al., 2010; Stokes et al., 1989). The thoracic region (T1–T5), which is fully in contact with the lung and exposed to the pulmonary forces, displayed minor abnormalities in bone formation. This supports the hypothesis that an asymmetrical growth disturbance is not the primary cause for AIS (Qiu et al., 2010; Zhu et al., 2011). The mechanical stimuli for increased bone formation and longer left caudal ribs may originate from asymmetrical muscle forces of the diaphragm and abdominal muscles (Kasai et al., 2002; Qiu et al., 2010; Stokes et al., 1989).

4.2 | Rib position and inclination

The rib cage of AIS patients exhibited large deformities with more medially oriented ribs on the left side, and more dorsally and laterally placed ribs on the right side. The data further indicate that the observed rib hump in AIS could result from a more ventral position of the ribs on the concave side, rather than a bulging of the ribs to the rib hump on the convex side.

All deformities were associated with a relative increase in the inflection angle of the ribs. Therefore, the rib cage appeared to respond consistently to spinal deformities by increasing the inflection angle of the ribs.

4.3 | Rib area

The calculated rib area represents the area that is enclosed by a rib within the chest. This area provides regional information on the potential space for the lung volume at each rib-level. The data showed that this area is closely related to the rib length. In the upper thoracic region (T1–T7), which is particularly relevant for the lung, no significant difference to the healthy group was found. It should be noted

that the size of the lung can expand beyond the rib area towards the costal cartilage and sternum.

4.4 | Lung volume

No statistical differences of the lung volume or the relationship between the left and right lung volumes were identified between the groups. However, the anatomical proximity of the pleura in AIS patients was found to be reduced on the right side and increased on the left side of the rib cage. This impairment was more pronounced with a greater spinal deformity. This is reasonable because the lung is not rigidly coupled with the ribs. A deviation in the anatomical proximity of the pleura between the left and right sides of the rib cage may change the intrapleural pressure distribution. To what extent this potential asymmetrical pressure distribution impacts the biomechanical integrity in scoliotic patients is unknown and needs further investigation.

Interestingly, three of the four thoracolumbar cases exhibited a detached lung locally in the area of T7 on the right (convex) posterior side of the rib cage. This may be associated with the occurrence of a pleural incidence, such as pneumonia, in some scoliotic patients (Banjar, 2003). To identify whether this pleural phenomenon occurs generally in these C-shaped curved spines requires further investigations with larger patient groups.

4.5 | Rib cage width to spinal length ratio

The presence of an anterior “overgrowth” of the anterior column within scoliotic spines has been generally acknowledged. It was quantified by measuring differences between the posterior and anterior heights of the spinal column (Porter, 2000; Schlösser et al., 2016). This overgrowth may be explained by the Hueter-Volkman principle (Stokes, 2002), which states that a mechanical compression/decompression across the growth plate decreases/increases the longitudinal growth. An open question remains whether

the height (straight line from T1 to T12) of the scoliotic spine is reduced or the length (line along the spinal curvature from T1 to T12) of the scoliotic spine is increased. This is particularly relevant when straightening the spine within a surgery.

According to the data of our study, the width of the rib cage at T6 appears normally developed in AIS patients. Therefore, we used the rib cage width in relation to the spinal length to determine whether a pathological condition was present. This ratio was interestingly nearly 1 in the healthy group. The thoracic AIS group displayed a significant increase in the width to height ratio. This would imply that the height of the scoliotic spine was reduced within the thoracic spinal group. Therefore, the data suggest that the spinal overgrowth theory does not compensate for the deformed curvature. Furthermore, the measured overgrowth in the literature may be due to a reduced posterior column and not primarily to an increased anterior column. Therefore, after straightening a scoliotic thoracic curvature, an AIS patient would gain normal height according to their growth.

In severe scoliosis cases, a rib costoplasty may be performed to reduce the rib hump and improve the cosmesis. According to the data in the present study, the length of the ribs in AIS patients appeared normally developed within the regions occupied by the lung. A reduction of the rib length may be problematic, because it would lead to a reduction of the pleural space and thus reduce the lung capacity. A reduction of the vital capacity of the lung after costoplasty was indeed reported (Harding et al., 2005). This is also relevant, because a rib hump correction may be compromised 2 years post-surgery (Pratt et al., 2001).

The primary limitation of this study was the small amount of patient data. In particular, the analysis of the thoracolumbar AIS group with $n = 4$ cannot be considered as representative. Due to ethical concerns, CT images in high quality, which cover the entire thoracic and lumbar spine, including the rib cage, are rarely taken. The obtained data make the analysed images within this study an exceptional database.

Sources of error also include the placement of the landmarks, specifically on the deformed scoliotic vertebrae and ribs. Therefore, only morphological parameters with marginal intra- and interrater variability were considered in the present study. The greatest deviation was documented for the 12th rib, because the expression of the 12th rib strongly deviated between patients. This error was reflected by the large standard deviation.

Commonly, patients take a big breath and hold it during a CT scan. However, no information on the respiratory condition of the patient during the CT acquisition was obtained. Therefore, the magnitude of the lung volumes should be viewed with caution, because these can vary during breathing. Nevertheless, the data on the relative lung volumes between the left and right sides could indicate fundamental abnormalities.

5 | CONCLUSIONS

Respiratory mechanics are an important aspect to be considered when evaluating morphological patterns of the rib cage in AIS. In combination

with the spinal curvature, the pleural mechanics appeared to have a strong impact on the shape of the rib cage. Despite the fact that the rib cage can be significantly deformed, the lungs and their encompassing ribs appeared normally developed in the AIS group.

ACKNOWLEDGMENTS

This work was supported by the German Research Foundation (DFG): Project WI 1352/20-2 and Project WI 1352/22-1.

AUTHOR CONTRIBUTION

Benedikt Schlager performed concept/design, acquisition of data, data analysis/interpretation, drafting of the manuscript. Florian Krump performed acquisition of data, data analysis & interpretation. Julius Boettinger performed acquisition of data, data analysis & interpretation. Rene Jonas performed data analysis, critical revision of the manuscript and approval of the article. Frank Niemeyer performed data analysis, critical revision of the manuscript and approval of the article. Christian Liebsch performed data interpretation, critical revision of the manuscript and approval of the article. Dr. Michael Ruf performed acquisition of data, critical revision of the manuscript and approval of the article. Prof. Meinrad Beer performed acquisition of data, critical revision of the manuscript and approval of the article. Prof. Dr. Hans-Joachim Wilke performed data interpretation, drafting of the manuscript, critical revision of the manuscript and approval of the article.

DATA AVAILABILITY STATEMENT

Data available on request due to privacy/ethical restrictions.

ORCID

Benedikt Schlager  <https://orcid.org/0000-0003-2371-851X>

Hans-Joachim Wilke  <https://orcid.org/0000-0001-6007-8844>

REFERENCES

- Abdelaal, A.A.M., Abd El Kafy, E.M.A.E.S., Elayat, M.S.E.M., Sabbahi, M. & Badghish, M.S.S. (2018) Changes in pulmonary function and functional capacity in adolescents with mild idiopathic scoliosis: observational cohort study. *Journal of International Medical Research*, 46, 381–391. <https://doi.org/10.1177/0300060517715375>
- Banjar, H.H. (2003) Pediatric scoliosis and the lung. *Saudi Medical Journal*, 24, 957–963.
- Bastir, M., García Martínez, D., Recheis, W., Barash, A., Coquerelle, M., Rios, L. et al. (2013) Differential growth and development of the upper and lower human thorax. *PLoS One*, 8, 1–13. <https://doi.org/10.1371/journal.pone.0075128>
- Bouloussa, H., Pietton, R., Vergari, C., Haen, T.X., Skalli, W. & Vialle, R. (2019) Biplanar stereoradiography predicts pulmonary function tests in adolescent idiopathic scoliosis: a cross-sectional study. *European Spine Journal*, 28, 1962–1969. <https://doi.org/10.1007/s00586-019-05940-3>
- Closkey, R.F. & Schultz, A.B. (1993) Rib cage deformities in scoliosis: spine morphology, rib cage stiffness, and tomography imaging. *Journal of Orthopaedic Research*, 11, 730–737. <https://doi.org/10.1002/jor.1100110515>
- Dreimann, M., Hoffmann, M., Kossow, K., Hitzl, W., Meier, O. & Koller, H. (2014) Scoliosis and chest cage deformity measures predicting impairments in pulmonary function. *Spine (Phila Pa 1976)*, 39, 2024–2033.

- Eberlein, M., Schmidt, G.A. & Brower, R.G. (2014) Chest wall strapping: an old physiology experiment with new relevance to small airways diseases. *Annals of the American Thoracic Society*, 11, 1258–1266. <https://doi.org/10.1513/AnnalsATS.201312-465O1>
- Gayzik, F.S., Yu, M.M., Danelson, K.A., Slice, D.E. & Stitzel, J.D. (2008) Quantification of age-related shape change of the human rib cage through geometric morphometrics. *Journal of Biomechanics*, 41, 1545–1554. <https://doi.org/10.1016/j.jbiomech.2008.02.006>
- Grivas, T.B., Burwell, R.G., Purdue, M., Webb, J.K. & Moulton, A. (1991) A segmental analysis of thoracic shape in chest radiographs of children. Changes related to spinal level, age, sex, side and significance for lung growth and scoliosis. *Journal of anatomy*, 178, 21–38.
- Grivas, T.B., Vasiliadis, E.S., Mihas, C. & Savvidou, O. (2007) The effect of growth on the correlation between the spinal and rib cage deformity: implications on idiopathic scoliosis pathogenesis. *Scoliosis*, 2, 11. <https://doi.org/10.1186/1748-7161-2-11>
- Harding, I.J., Chopin, D., Charosky, S., Vialle, R., Carrizo, D. & Delecourt, C. (2005) Long-term results of Schollner costoplasty in patients with idiopathic scoliosis. *Spine (Phila Pa 1976)*, 30, 1627–1631.
- Harris, J.A., Mayer, O.H., Shah, S.A., Campbell, R.M. & Balasubramanian, S. (2014) A comprehensive review of thoracic deformity parameters in scoliosis. *European Spine Journal*, 23, 2594–2602. <https://doi.org/10.1007/s00586-014-3580-8>
- Holcombe, S.A., Wang, S.C. & Grotberg, J.B. (2017) The effect of age and demographics on rib shape. *Journal of Anatomy*, 231, 229–247. <https://doi.org/10.1111/joa.12632>
- Kasai, Y., Takegami, K. & Uchida, A. (2002) Length of the ribs in patients with idiopathic scoliosis. *Archives of Orthopaedic and Trauma Surgery*, 122, 161–162. <https://doi.org/10.1007/s00402-001-0357-4>
- Kearon, C., Viviani, G.R., Kirkley, A. & Killian, K.J. (1993) Factors determining pulmonary function in adolescent idiopathic thoracic scoliosis. *American Review of Respiratory Disease*, 148, 288–294. <https://doi.org/10.1164/ajrccm/148.2.288>
- Kotani, T., Minami, S., Takahashi, K., Isobe, K., Nakata, Y., Takaso, M. et al. (2004) An analysis of chest wall and diaphragm motions in patients with idiopathic scoliosis using dynamic breathing MRI. *Spine (Phila Pa 1976)*, 29, 298–302.
- Labelle, H., Dansereau, J., Bellefleur, C. & Jéquier, J.C. (1995) Variability of geometric measurements from three-dimensional reconstructions of scoliotic spines and rib cages. *European Spine Journal*, 4, 88–94. <https://doi.org/10.1007/BF00278918>
- Leong, J.C.Y., Lu, W.W., Luk, K.D.K. & Karlberg, E.M. (1999) Kinematics of the chest cage and spine during breathing in healthy individuals and in patients with adolescent idiopathic scoliosis. *Spine (Phila Pa 1976)*, 24, 1310–1315.
- Liebsch, C., Graf, N., Appelt, K. & Wilke, H.-J. (2017) The rib cage stabilizes the human thoracic spine: an in vitro study using stepwise reduction of rib cage structures. *PLoS One*, 12, e0178733. <https://doi.org/10.1371/journal.pone.0178733>
- Liebsch, C., Graf, N. & Wilke, H.-J. (2019) In vitro analysis of kinematics and elastostatics of the human rib cage during thoracic spinal movement for the validation of numerical models. *Journal of Biomechanics*, 94, 147–157. <https://doi.org/10.1016/j.jbiomech.2019.07.041>
- Liebsch, C. & Wilke, H.-J. (2020) Rib presence, anterior rib cage integrity, and segmental length affect the stability of the human thoracic spine: an in vitro study. *Front Bioeng Biotechnol*, 8, 1–10. <https://doi.org/10.3389/fbioe.2020.00046>
- Okuno, K., Ishizu, K., Matsubayashi, J., Fujii, S., Sakamoto, R., Ishikawa, A. et al. (2019) Rib cage morphogenesis in the human embryo: a detailed three-dimensional analysis. *Anatomical Record*, 302, 2211–2223. <https://doi.org/10.1002/ar.24226>
- Openshaw, P., Edwards, S. & Helms, P. (1984) Changes in rib cage geometry during childhood. *Thorax*, 39, 624–627. <https://doi.org/10.1136/thx.39.8.624>
- Parent, S., Labelle, H., Skalli, W., Latimer, B. & de Guise, J. (2002) Morphometric analysis of anatomic scoliotic specimens. *Spine (Phila Pa 1976)*, 27, 2305–2311.
- Porter, R. (2000) Idiopathic scoliosis: the relation between the vertebral canal and the vertebral bodies. *Spine (Phila Pa 1976)*, 25, 1360–1366. <https://doi.org/10.1097/00007632-200006010-00007>
- Pratt, R.K., Webb, J.K., Burwell, R.G. & Cole, A.A. (2001) Changes in surface and radiographic deformity after Universal Spine System for right thoracic adolescent idiopathic scoliosis: is rib-hump reassertion a mechanical problem of the thoracic cage rather than an effect of relative anterior spinal overgrowth? *Spine (Phila Pa 1976)*, 26, 1778–1787.
- Qiu, Y., Sun, G., Zhu, F., Wang, W. & Zhu, Z. (2010) Rib length discrepancy in patients with adolescent idiopathic scoliosis. *Studies in Health Technology and Informatics*, 158, 63–66.
- Sanchis-Gimeno, J.A., Lois-Zlolniski, S., María González-Ruiz, J., Palancar, C.A., Torres-Tamayo, N., García-Martínez, D. et al. (2020) Association between ribs shape and pulmonary function in patients with Osteogenesis Imperfecta. *Journal of Advanced Research*, 21, 177–185. <https://doi.org/10.1016/j.jare.2019.10.007>
- Schlager, B., Krump, F., Boettinger, J., Niemeier, F., Ruf, M., Kleiner, S. et al. (2018) Characteristic morphological patterns within adolescent idiopathic scoliosis may be explained by mechanical loading. *European Spine Journal*, 27, 2184–2191. <https://doi.org/10.1007/s00586-018-5622-0>
- Schlösser, T.P.C., Van Stralen, M., Chu, W.C.W., Lam, T.P., Ng, B.K.W., Vincken, K.L. et al. (2016) Anterior overgrowth in primary curves, compensatory curves and junctional segments in adolescent idiopathic scoliosis. *PLoS One*, 11, 1–11. <https://doi.org/10.1371/journal.pone.0160267>
- Smyth, R.J., Chapman, K.R., Wright, T.A., Crawford, J.S. & Rebeck, A.S. (1984) Pulmonary function in adolescents with mild idiopathic scoliosis. *Thorax*, 39, 901–904. <https://doi.org/10.1136/thx.39.12.901>
- Stokes, I.A.F. (2002) Mechanical effects on skeletal growth. *Journal of Musculoskeletal and Neuronal Interactions*, 2, 277–280.
- Stokes, I.A.F., Dansereau, J. & Moreland, M.S. (1989) Rib cage asymmetry in idiopathic scoliosis. *Journal of Orthopaedic Research*, 7, 599–606. <https://doi.org/10.1002/jor.1100070419>
- Stokes, I.A., Spence, H., Aronsson, D.D. & Kilmer, N. (1996) Mechanical modulation of vertebral body growth. Implications for scoliosis progression. *Spine (Phila Pa 1976)*, 21, 1162–1167.
- Virtanen, P., Gommers, R., Oliphant, T.E., Haberland, M., Reddy, T., Cournapeau, D. et al. (2020) SciPy 1.0: fundamental algorithms for scientific computing in Python. *Nature Methods*, 17, 261–272. <https://doi.org/10.1038/s41592-019-0686-2>
- Yaszay, B., Bastrom, T.P., Bartley, C.E., Parent, S. & Newton, P.O. (2017) The effects of the three-dimensional deformity of adolescent idiopathic scoliosis on pulmonary function. *European Spine Journal*, 26, 1658–1664. <https://doi.org/10.1007/s00586-016-4694-y>
- Zhu, F., Chu, W.C., Sun, G. & Wang, Z.Z.W. (2011) Rib length asymmetry in thoracic adolescent idiopathic scoliosis: is it primary or secondary? *European Spine Journal*, 20, 254–259.

How to cite this article: Schlager, B., Krump, F., Boettinger, J., Jonas, R., Liebsch, C., Ruf, M. et al. (2022) Morphological patterns of the rib cage and lung in the healthy and adolescent idiopathic scoliosis. *Journal of Anatomy*, 240, 120–130. <https://doi.org/10.1111/joa.13528>

APPENDIX

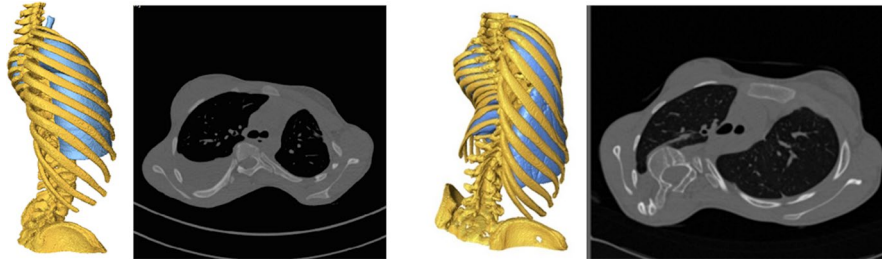


Figure A1 Example CT images with the 3D-reconstruction of two thoracolumbar AIS cases, which display an offset of the lung (blue) in the posterior region of the rib cage on the convex side of the spinal curvature